Journal of Industrial and Engineering Chemistry xxx (2016) xxx–xxx

Contents lists available at ScienceDirect

Journal of Industrial and Engineering Chemistry

journal homepage: www.elsevier.com/locate/jiec

Controlled pH- and glucose-responsive drug release behavior of cationic chitosan based nano-composite hydrogels by using graphene oxide as drug nanocarrier

Xiaowen Zhao, Xue Zou, Lin Ye*

State Key Laboratory of Polymer Materials Engineering, Polymer Research Institute of Sichuan University, Chengdu 610065, China

ARTICLE INFO

Article history:
Received 26 October 2016
Received in revised form 13 December 2016
Accepted 25 December 2016
Available online xxx

Keywords:
Cationic chitosan
Graphene oxide (GO)
Drug nano-carrier
pH-/glucose-sensitivity
Initial burst release

ABSTRACT

To realize tight control of hyperglycemia for diabetic patients, cationic chitosan (HTCC) based nano-composite hydrogels were prepared by using graphene oxide (GO) as nano-carrier for the model drug (bovine serum albumin, BSA). BSA intercalated into the layers of GO and the intercalation process was mainly driven by the mutual electrostatic interaction. By introducing GO-BSA, a more compact GO-centered network structure formed for the hydrogel. Compared with HTCC/BSA, HTCC/2.0wt%GO-BSA hydrogels exhibited a more distinct pH-/glucose-sensitivity and a much lower initial burst release, which was attributed to the compact structure and strong interactions among HTCC, GO and BSA in the hydrogel system.

Introduction

Diabetes mellitus, a disorder of glucose regulation, is a global burden affecting 366 million people across the world [1]. For tight control of hyperglycemia and prevention of the resulting complications in diabetic patients, it is highly desirable to develop simple, effective, and continuously self-regulated drug delivery systems [2]. Glucose-responsive hydrogels, known as stimuli-responsive or "intelligent" systems, can adapt the rate of drug release in response to changes in glucose concentration in order to maintain blood glucose levels within the normal range. Enzyme glucose oxidase (GOD), a widely used natural receptor, can be entrapped or immobilized within a pH-sensitive matrix, which results in enzyme-catalyzed conversion of glucose to gluconic acid, thereby lowering the pH in the microenvironment of the hydrogel and causing drug release [3–5].

Chitosan (CS), a copolymer of D-glucosamine and *N*-acetylglucosamine derived from chitin, is a potentially useful pharmaceutical material owing to its good biocompatibility and low toxicity [6,7]. In our previous study, it was demonstrated that chitosan microspheres based on the amino group were pH-sensitive in a wide range of pH 1.0–9.0, which was not suitable in the field of glucose responsive drug release systems with a narrow physiological pH-sensitive variation range from 7.4 to 6.8 for the conversion of glucose to gluconic acid through GOD [8]. Meanwhile the cationic chitosan (HTCC) synthesized by grafting with glycidyltrimethylammonium chloride (GTMAC) showed more distinct pH sensitivity as compared with chitosan and satisfied the above mentioned narrow physiological pH variation for glucose responsive drug release systems [9]. However, the initial burst effect was the main problems for the application of such HTCC hydrogels systems. The burst release of drugs is usually due to the weak interaction between polymer matrix and drugs, and the quick swollen rate of the polymer gel during the initial release process.

Recently, the preparation and application of novel biopolymer/nanomaterial composites [10–12] as controlled drug delivery vehicles have attracted much attention owing to their unique structure and properties. Graphene oxide (GO), an oxidative derivative of graphene, has attracted extensive interests in drug delivery. GO sheets are enriched with oxygen-containing functional groups such as hydroxyl and epoxy group on the basal planes and carbonyl and carboxylic groups at the sheet edges. Thus, the GO sheets with one-atom thickness and two-dimensional plane structure can provide large specific surface area to carry drugs via surface adsorption, hydrogen bonding, and other types of interactions [13], which makes it a promising material for drug carrier [14–21].

Very limited works have been published regarding the use of CS/GO nano-composites for drug delivery. Justin and Ben [22]

* Corresponding author. Fax: +86 28 85402465.
E-mail address: yelinwh@126.com (L. Ye).

http://dx.doi.org/10.1016/j.jiec.2016.12.023
1226-086X/

studied the drug release behavior of CS/GO nano-composite film, which offered a faster and a more substantial release of drug than CS, and the pH-sensitive release functionality of the nano-composite was also demonstrated, releasing 48% less drug in an acidic condition than that in a neutral environment. Chen et al. [23] prepared a series of porous CS/GO composite xerogels, which can absorb and slowly release an anticancer drug, doxorubicin hydrochloride (DOX). The cumulative release percentage of DOX from the xerogels at pH 4 was much higher than that at pH 7.4. In summary, for the current reported intelligent CS/GO drug release systems, the pH-sensitive variation range was too wide to satisfy the glucose-responsive drug release systems. And up to now, no literature can be available for the effect of GO on the glucose-responsive drug release behavior of CS.

In this study, GO was used as nanocarrier for bovine serum albumin (BSA) as the model drug. A series of GO-BSA intercalation complexes were prepared at first, and then, by using the cationic chitosan (HTCC) prepared in our previous study as the pH-sensitive polymer matrix and enzyme glucose oxidase (GOD) as the glucose-sensitive receptor, GO-BSA loaded intelligent hydrogels (HTCC/GO-BSA) were prepared. The intercalation behavior of GO-BSA was studied, and the network structures as well as pH- and glucose-responsive drug release behavior of HTCC/GO-BSA hydrogels were investigated.

Experimental

Materials

Chitosan (molecular weight 1×10^6 Da, degree of deacetylation 85%) was purchased from Zhejiang Jinke Biochemical Co. Ltd. (Zhejiang, China). Epichlorohydrin and sodium tripolyphosphate (TPP) were purchased from Tianjin Tianda Chemical Reagent Co. (Tianjin, China). Glycidyltrimethylammonium chloride (GTMAC) was obtained from Dongyingguofeng Fine Chemical Co. Ltd. (Shandong, China). Bovine serum albumin (BSA) was provided by Huayi Bioengineering Co. Ltd. (Hubei, China). Glucose, enzyme glucose oxidase (GOD) and insulin were purchased from Baoxin Biotechnology Co. Ltd. (Chengdu, China). All other reagents were of analytic reagent grade. Double distilled water was used throughout.

Preparation of GO-BSA intercalation complexes

The preparation procedure for the GO-BSA intercalation complexes was carried out as follows: 0.5 g of GO was dispersed in 200 ml of deionized water under ultrasound for 30 min at room temperature, and in this process the stable GO/H_2O dispersion solution formed. Then BSA was added and the mixture solution was stirred for another 4 h. Afterwards, GO-BSA dispersion solution was centrifugated and washed with distilled water to remove the free BSA. The resulting solids were freeze-dried for 12 h, finally yielding GO-BSA intercalation complexes.

Preparation of HTCC/GO nano-composite hydrogels

Chitosan was dispersed in water/isopropanol media at 37 °C and stirred for 30 min prior to dropwise addition of GTMAC. Then the reaction mixture was stirred at 60 °C for another 6 h. After being precipitated and washed with cold acetone, cationic chitosan (HTCC) was obtained by filtration.

Afterwards, HTCC with GO-BSA and GOD was dissolved in distilled water at room temperature and crosslinking agent (TPP) was added. After incubating at 37 °C for 2 h, HTCC/GO-BSA hydrogels formed. The samples were freeze-dried for 24 h and stored at 4 °C before use.

Measurements

X-ray diffraction analysis (XRD)

The interlayer spacing of the samples of GO and GO-BSA was measured at room temperature over the scanning range of $2\theta = 3$–20° with Rigaku D/max III B x-ray diffraction equipment (Japan). Copper (Cu) K_α radiation ($\lambda = 0.154$ nm) was used at a generator voltage of 40 kV, current of 35 mA, and the scanning speed was 2.4 deg min^{-1}. The d-spacing of the GO-BSA layers was calculated with the Bragg equation:

$$2d\sin\theta = n\lambda \quad (1)$$

where θ is the diffraction angle; n is the order of diffraction, and λ is the incident wavelength.

Thermo-gravimetric analysis (TGA)

The thermo-gravimetric analysis (TGA) was used to characterize the thermal stability and intercalation ratio of GO-BSA. TGA was performed with a TA2950 thermo-balance from TA Co. (USA) under nitrogen atmosphere with the flow rate of 50 ml/min. The granulated samples of about 10 mg were heated from ambient temperature to approximately 800 °C at a heating rate of 10 °C/min.

Atomic force microscopy (AFM)

The surface morphologies and thickness of GO and GO-BSA were examined by AFM. The AFM measurements were performed with a SPM-9700 Scanning Probe Microscope (Japan) in a tapping mode from Digital Instruments with a Nanoscope IV controller. Samples for AFM imaging were prepared by drop-casting the GO and GO-BSA dispersions onto freshly cleaved mica substrates, which were then allowed to dry in air at ambient temperature and pressure.

Scanning electron microscopy analysis (SEM)

The morphology of the fractured surface of HTCC/GO-BSA hydrogels was observed with a JEOL JSM-5900LV scanning electron microscopy (SEM) (Japan). The operating voltage was 5 kV. The samples were ion beam sputter-coated with gold and the thin layer thickness was about 1–20 nm.

Transmission electron microscopy analysis (TEM)

The morphologies of GO-BSA intercalation complexes were observed with a Titan G2 60-300 transmission electron microscopy (TEM) (U.S.A.) at an accelerating voltage of 300 kV. Samples were dispersed in distilled water and dropped onto 200-mesh copper grids for TEM observation.

Rheological behavior

The visco-elasticity behaviors of HTCC/GO-BSA hydrogels were analyzed with Rheometer System Gemini 200 of Malvern Instrument Co. (UK), using parallel plates with 25 mm diameter and 1–2 mm plate-to-plate distance. For the strain scan experiment, the shear elastic modulus (G′) and viscous modulus (G″) were measured at 0.01–100% strain and 1 Hz frequency. For the frequency scan experiment, G′ and G″ were measured in the linear visco-elastic region, at 0.01–100 Hz frequency and 0.1% maximum strain.

Swelling ratio

The swelling properties of the HTCC/GO-BSA hydrogels were investigated in phosphate buffered saline (PBS) with pH 6.8. Hydrogels of a known weight (W_0) were immersed in PBS buffer solutions at 37 °C. Then, the hydrogels were taken out at predetermined intervals and weighed after removing excess solution on the surface. The swelling ratio can be determined

Please cite this article in press as: X. Zhao, et al., Controlled pH- and glucose-responsive drug release behavior of cationic chitosan based nano-composite hydrogels by using graphene oxide as drug nanocarrier, J. Ind. Eng. Chem. (2016), http://dx.doi.org/10.1016/j.jiec.2016.12.023

using Eq. (2):

$$\text{Swelling ratio}(\%) = (W_t - W_0) * 100\%/W_o \quad (2)$$

where W_0 is the dried weight of hydrogels and W_t is the weight of the hydrated hydrogels at time t.

In vitro drug release

In vitro pH-sensitive drug release testing was carried out by incubating 10 mg HTCC/GO-BSA hydrogels samples in PBS buffer solutions with pH values of 6.8 and 7.4. Glucose-sensitive drug release behavior was analyzed by incubating 10 mg HTCC/GO-BSA hydrogels samples in PBS buffer solutions (pH 7.4) with glucose concentration values of 0, 1, 4 mg ml^{-1}. At specified time intervals, 2 ml of this solution was taken out and assayed by an Alpha-1860 UV spectrometer (China) at the wavelength of 214 nm. The amount of BSA released from the testing hydrogels was then calculated from the standard BSA calibration curve. Samples in triplicate were averaged for each experiment.

The cumulative release (%) was determined using Eq. (3):

$$\text{Cumulative release}(\%) = \frac{V_c\sum_{i=1}^{n-1} C_i + V_o C_n}{W_o} \times 100\% \quad (3)$$

where V_e is the replaced volume of PBS buffer (2 ml); V_0 is the total volume of PBS buffer (10 ml); C_i and C_n are the drug release concentrations (mg ml^{-1}) at different times, and W_o is the amount of the drug loaded onto the hydrogels (mg).

Statistical analysis

The quantitative results were obtained from triplicate samples and the data were expressed as mean ± SD (n = 3). Statistical analysis was performed using one-way analysis of variance, followed by post hoc Student's *t*-test. A value of $p < 0.05$ was considered to be statistically significant.

Results and discussion

Intercalation behavior of GO-BSA complexes

GO-BSA complexes with varying mass ratio of BSA/GO were prepared. The mass ratio of BSA/GO was 0.5:1, 1:1, 2:1, 4:1, 8:1 and 10:1 respectively, which was denoted as GO-BSA-1, GO-BSA-2, GO-BSA-3, GO-BSA-4, GO-BSA-5 and GO-BSA-6.

The XRD patterns of GO and GO-BSA were shown in Fig. 1. For GO, the sharp characteristic peak for the (002) plane of GO could be observed at $2\theta = 11.25°$, corresponding to the interlayer spacing of 0.7856 nm. It was significantly larger than that of the pristine graphite ($2\theta = 26.6°$, corresponding to a d-spacing of 0.336 nm), due to the intercalation of oxide functional groups. For GO-BSA-1, the peak shifted to $2\theta = 9.92°$, corresponding to $d_{002} = 0.8953$ nm. The increase of the interlayer spacing of (002) plane of GO can be attributed to the intercalated BSA chains in the interlayer space of GO. With the increase of BSA/GO mass ratio, the d_{002} values increased, and when the mass ratio of BSA/GO increased to 8:1 and 10:1, the value of d_{002} reached the maximum of about 1.08 nm and remained almost constant, as shown in Fig. 2.

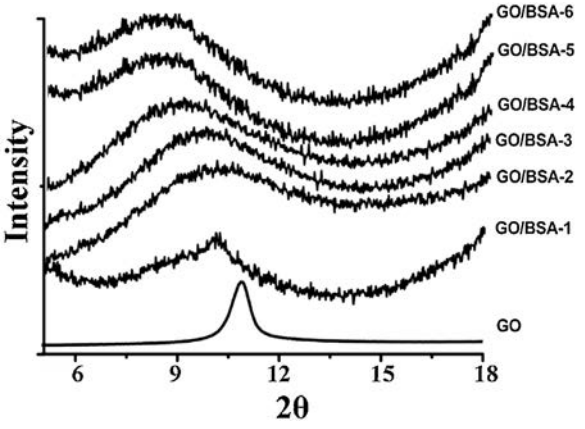

Fig. 1. XRD patterns of GO and GO-BSA with varying BSA/GO mass ratio.

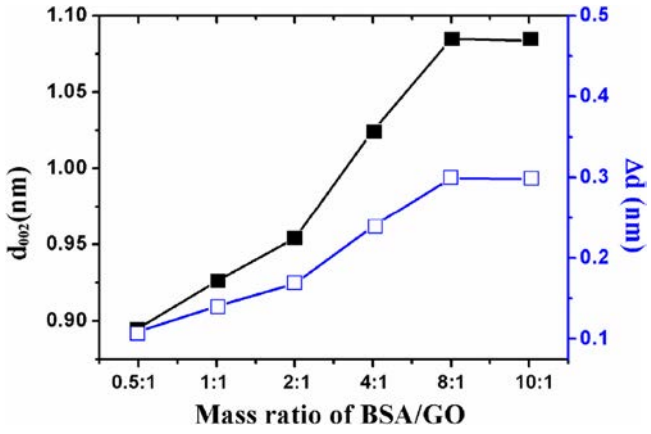

Fig. 2. d_{002} and Δd values of GO-BSA with varying BSA/GO mass ratio.

Relative to the interlayer spacing of GO (0.7856 nm), the increase of the interlayer spacing corresponded to the thickness of the intercalated BSA chains (Δd). The thickness of the intercalated BSA molecular chains (Δd) of GO-BSA based on the XRD results was also shown in Fig. 2. It can be seen that with the increase of BSA/GO mass ratio, the Δd values first increased, reaching the maximum at the BSA/GO mass ratio of 8:1 for GO-BSA-5, and then remained constant, which indicated that there was a saturation content when BSA intercalated GO.

TGA curves of GO and GO-BSA with varying mass ratio of BSA/GO were shown in Fig. 3. For GO, it showed a weight loss of 15.46% below 110 °C, attributed to the removal of the water held in the interlayer. A second large weight loss was observed in the range of 110–300 °C due to the removal of functional groups of —OH, —COOH from GO layer, leaving residual carbon. For GO-BSA hybrids, obvious weight loss during 210–400 °C can be observed due to the degradation of BSA chains. The TGA curve of GO-BSA-1

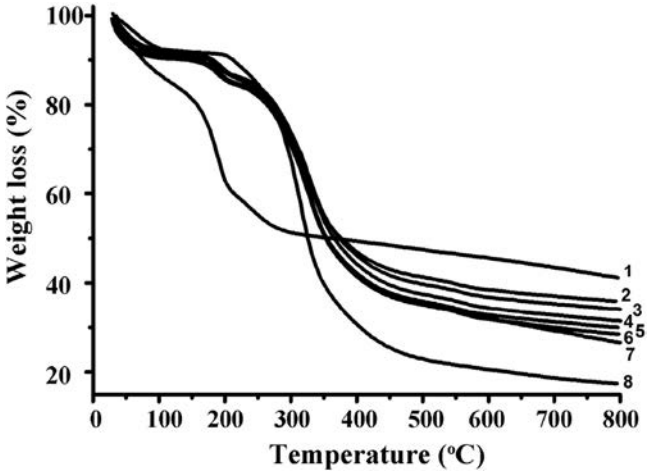

Fig. 3. TGA curves of GO and GO-BSA (1 – GO; 2 – GO-BSA-1; 3 – GO-BSA-2; 4 – GO-BSA-3; 5 – GO-BSA-4; 6 – GO-BSA-5; 7 – GO-BSA-6; 8 – BSA).

Please cite this article in press as: X. Zhao, et al., Controlled pH- and glucose-responsive drug release behavior of cationic chitosan based nanocomposite hydrogels by using graphene oxide as drug nanocarrier, J. Ind. Eng. Chem. (2016), http://dx.doi.org/10.1016/j.jiec.2016.12.023

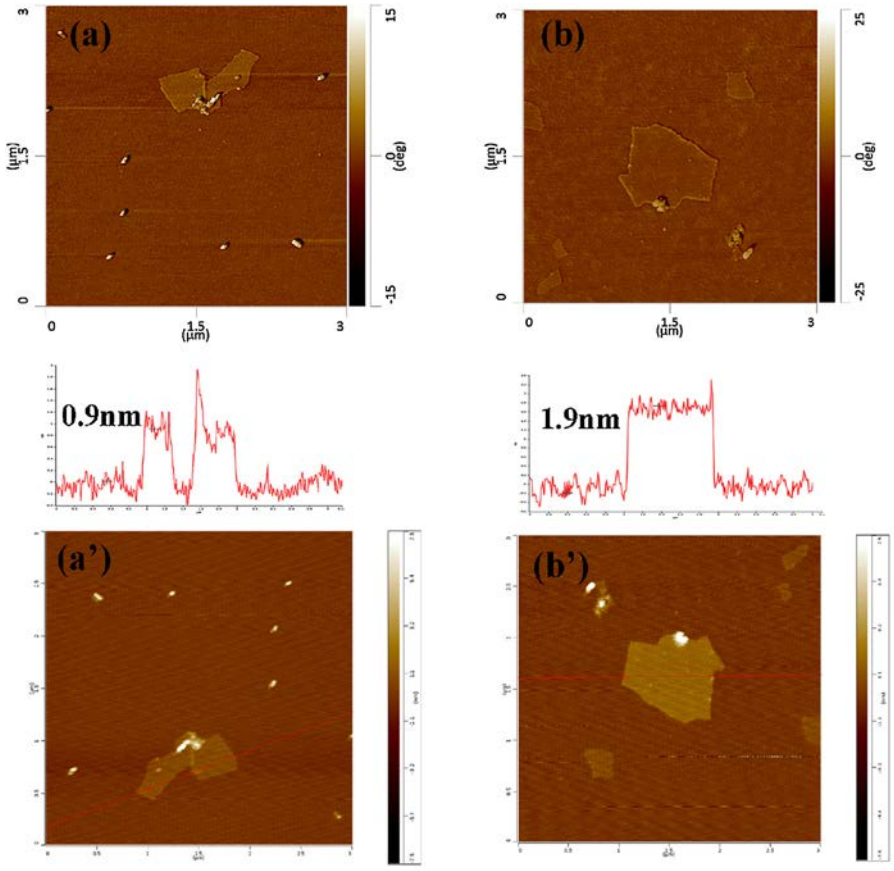

Fig. 4. Typical tapping-mode AFM images of (a) GO, (b) GO-BSA and 3D view images of (a') GO, (b') GO-BSA.

(curve 2) showed a total of 70% weight loss in the whole temperature range, and with the increase of the BSA content, the weight loss increased indicating that the intercalated BSA molecules in the GO layers increased.

The mass percent of the intercalated BSA molecules in the unit mass of GO (per gram) can be calculated according to the TGA data.

$$M_1 = M_0 * W_{GO-BSA} - (M_0 - M_1) * W_{GO} \quad (4)$$

$$\text{that is, } M_1 = \frac{W_{GO-BSA} - W_{GO}}{1 - W_{GO}} * M_0 \quad (5)$$

$$D_1 = M_1/(M_0 - M_1) * 100\% \quad (6)$$

where W_{GO} and $W_{GO\text{-}BSA}$ are the residual ratio of thermal loss of GO and GO-BSA, respectively; M_1 is the mass of BSA intercalated in the GO layers; M_0 is the mass of the added GO-BSA; D_1 is the intercalation ratio of BSA molecules for per gram of GO.

The intercalation mass (M_1) and intercalation ratio (D_1) of BSA molecules in GO layers calculated according to Eqs. (4)–(6) were shown in Table 1. With increasing mass ratio of BSA/GO, the intercalation ratio (D_1) of GO-BSA first increased, and then maintained almost constant, reaching the maximum and saturation as high as 85.24% for GO-BSA-5, which was consistent with the XRD data.

Fig. 4 showed the typical AFM images and their 3D view images of GO and GO-BSA samples. For GO, the thickness of the individual nano-sheet was about of 0.9 nm, while for GO-BSA sample, the thickness increased to ~1.9 nm due to the binding of BSA molecules onto GO surface. Moreover, it was noticeable that the BSA molecular chains covered the whole plane of GO surface with relatively even height, indicating that BSA molecules were absorbed onto the GO surface homogeneously.

The dispersion state of GO in BSA was observed by TEM, as shown in Fig. 5. It can be seen that most of the GO layers, corresponding to the dark flakes, were well distributed in the BSA matrix.

BSA is a kind of globular protein consisting of a single peptide chain with 583 amino acids. It can be loaded on a variety of substrates which contain cations, anions, amino acids and so on. Therefore, the adsorption process of BSA onto the GO layers was mainly driven by the mutual electrostatic interaction between negatively charged GO sheets and positively charged —NH_2 group on BSA chains, together with some hydrogen bonding, as shown in Fig. 6.

Network structure of HTCC/GO-BSA hydrogel

By using HTCC as pH-sensitive polymer matrix, GOD as glucose-sensitive receptor and TPP as cross-linking agent, GO-BSA-5 loaded

Table 1
Thermal analysis data of GO and GO-BSA complexes.

Samples	M_0 (mg)	W (%)	M_1 (mg)	D_1 (%)
GO	3.8	58.84	–	–
GO-BSA-1	2.8	70.00	0.76	37.20
GO-BSA-2	1.8	70.74	0.52	40.67
GO-BSA-3	2.4	73.10	0.83	53.01
GO-BSA-4	1.6	75.61	0.65	68.76
GO-BSA-5	1.9	77.78	0.87	85.24
GO-BSA-6	1.4	77.76	0.64	85.07

Please cite this article in press as: X. Zhao, et al., Controlled pH- and glucose-responsive drug release behavior of cationic chitosan based nanocomposite hydrogels by using graphene oxide as drug nanocarrier, J. Ind. Eng. Chem. (2016), http://dx.doi.org/10.1016/j.jiec.2016.12.023

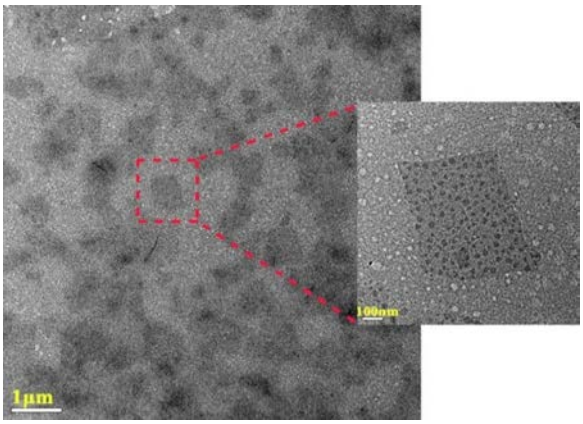

Fig. 5. TEM image of GO-BSA.

intelligent hydrogels were prepared. The added content of GO-BSA-5 was 0.5 wt%, 1.0 wt%, 1.5 wt%, and 2.0 wt% respectively, denoted as HTCC-XGO-BSA (X was the weight percent of GO-BSA-5). For comparison, sample of HTCC loaded with BSA was also prepared (denoted as HTCC/BSA).

Fig. 7(a) showed the strain dependence of the shear storage modulus, G′, and loss modulus, G″ at the frequency of 1 Hz for HTCC/GO-BSA hydrogels with different content of GO-BSA. At low strain amplitudes, the loss modulus of all hydrogels was lower than the storage modulus, which was consistent with the existence of a network structure. Meanwhile, at small strain amplitudes, G′ was independent of the strain amplitude, which indicated that the deformation imposed on the network structure was entirely reversible.

The frequency dependence of G′ and G″ was plotted in Fig. 7(b and c) for HTCC/GO-BSA. It can be seen that the value of G′ was larger than G″ and approximately independent of the test frequency in the range between 0.1 and 100 Hz for all the gel samples, showing that the elastic behavior of these samples predominated over their viscous behavior, and a perfect network formed. Moreover, it can be noted that, the modulus of the HTCC/GO-BSA hydrogels increased with the increase of GO-BSA content.

Based on the theory of Chambon and Winter [24], the strength (or stiffness) and structure of gelled systems can be evaluated by a constitutive equation [25,26]:

$$G(t) = St^{-n} \text{ for } \lambda_0 < t < \infty \quad (7)$$

where S is the gel stiffness; n is the critical network relaxation exponent and λ_0 corresponds to the relaxation time of transition to glassy state.

G′ and G″ of a critical gel follow an analogous power law:

$$G' = G''/\tan\delta = S\omega^n\Gamma(1-n)\cos\delta \quad (8)$$

where $\Gamma(1-n)$ is the gamma function and the network relaxation exponent n may be given by:

$$\delta = n\pi/2 (0 < n < 1) \quad (9)$$

A gel described by n approaching 1 is predominantly viscous, whereas one described by n approaching 0 behaves elastically. For all HTCC/GO-BSA hydrogels, n values, which were calculated from values of tan δ in Fig. 7 (d), approached 0, indicating a dominant elastic property and strong network structure.

In the hypothesis that the hydrogels may be regarded as a classic network, despite the fact that they presented a complex hierarchical structure, the storage modulus (G′) determined at low frequency may be related to the average number of equivalent units in a "network strand", N, connecting two "ideal" junctions and to approximate this, the value of the network mesh size L_c was calculated with Eqs. (10) and (11) [27]. Moreover, the crosslinking density (X) of hydrogels can be calculated with Eq. (12).

$$G' = RT\Phi^{1/3}/N_{AV}a^3N \quad (10)$$

$$L_c = (\Phi)^{-1/3}(C_\infty N)^{1/2}a \quad (11)$$

$$X = G'Q^{1/3}RT \quad (12)$$

In Eq. (10), G′ is the shear modulus of the hydrogels; R is the gas constant; T is the absolute temperature; Φ is the polymer volume fractions of gel in the swollen state; N_{AV} is Avogadro's number; $N_{AV}a^3$ is the molar volume of the solvent; N is the average number of equivalent units with volume equal to the solvent volume (a^3) between two junctions (in a "network strand"). In Eq. (11), C_∞ is the characteristic ratio of HTCC in relation to the molecular weight. In Eq. (12), Q is the equilibrium swelling ratio of HTCC hydrogels.

As shown in Table 2, the values of L_c obtained were in the range of 3.101–6.149 nm. With increasing GO-BSA content, G′ increased, L_c decreased, and the crosslinking density (X) of hydrogels

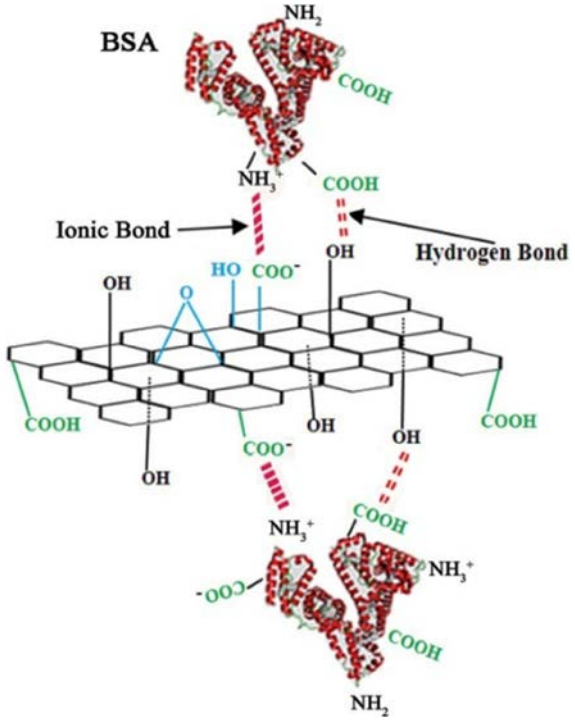

Fig. 6. Schematic diagram of interaction between GO and BSA.

Table 2
The network parameters of HTCC/GO-BSA hydrogels with different GO-BSA content.

Samples	G′ (Pa)	n	Φ	N	X (mol/cm^3)	L_c (nm)
HTCC/BSA	523,000	0.686	0.163	10.923	0.151	6.149
HTCC/0.5 wt%GO-BSA	563,000	0.637	0.169	10.431	0.163	5.920
HTCC/1.0 wt%GO-BSA	716,000	0.614	0.188	8.155	0.199	4.853
HTCC/1.5 wt%GO-BSA	979,000	0.564	0.199	5.918	0.264	3.809
HTCC/2.0 wt%GO-BSA	129,0000	0.521	0.209	4.468	0.342	3.101

Please cite this article in press as: X. Zhao, et al., Controlled pH- and glucose-responsive drug release behavior of cationic chitosan based nanocomposite hydrogels by using graphene oxide as drug nanocarrier, J. Ind. Eng. Chem. (2016), http://dx.doi.org/10.1016/j.jiec.2016.12.023

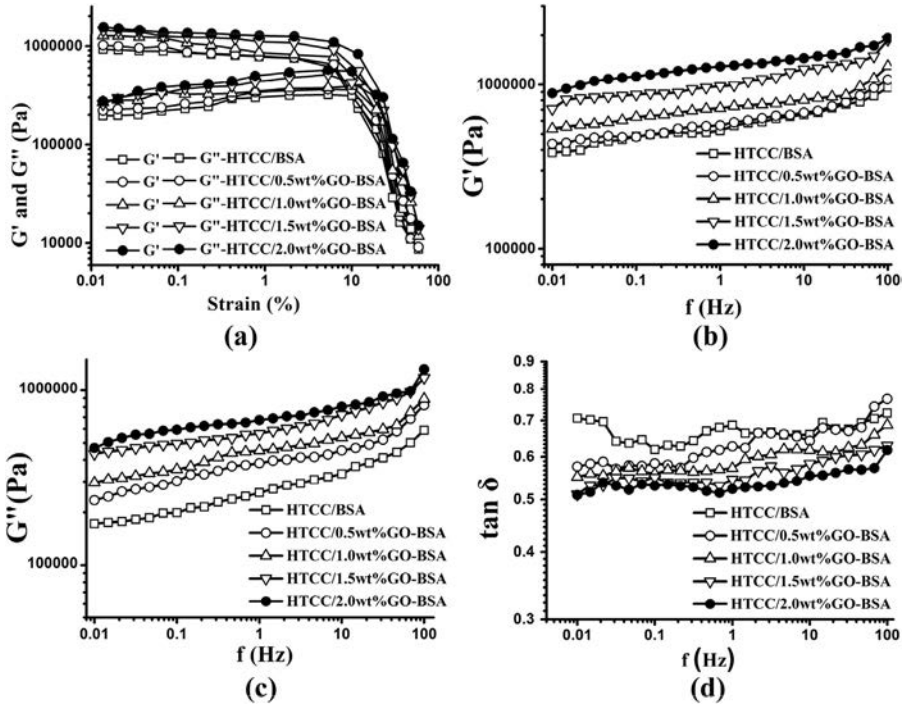

Fig. 7. G′, G″ and tan δ as a function of strain and frequency for HTCC/GO-BSA hydrogels with different GO-BSA content.

increased, due to the strong hydrogen bonding and electrostatic interactions between —COOH/—OH group on GO and —NH_2 group on HTCC, resulting in the formation of a more compact GO-centered network structure, as shown in Fig. 8.

The morphology of HTCC/BSA and HTCC/2.0 wt%GO-BSA hydrogels was observed by SEM as shown in Fig. 9. It can be seen that both hydrogels presented a porous structure. By introduction of GO, the size of pores in the hydrogel decreased obviously and a more compact network structure can be observed for HTCC/2.0 wt %GO-BSA hydrogels. Moreover, as shown in Fig. 9(c), GO-BSA sheets dispersed uniformly in the HTCC matrix without apparent defects or flaws, suggesting the strong interfacial interaction between HTCC and GO-BSA layers.

The swelling behavior of HTCC/GO-BSA with different GO-BSA content in buffer solutions (pH 6.8) was studied. As shown in Fig. 10, in the initial swelling stage, all samples absorbed water rapidly. And then the swelling ratio increased gradually with time, and reached equilibrium in about 12 h. The swelling ratios of HTCC/GO-BSA hydrogels decreased with increasing GO-BSA content, which was attributed to the higher crosslinking density

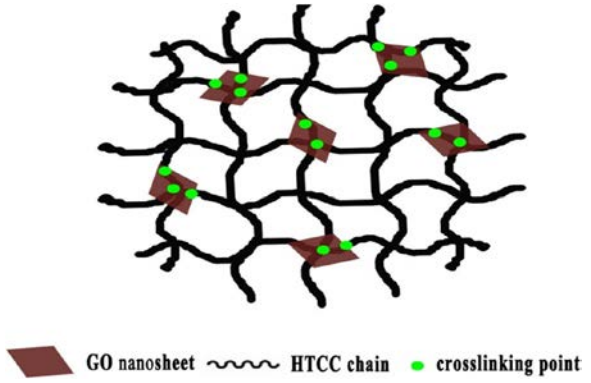

Fig. 8. The schematic representation of the crosslinking network structure of the HTCC/GO-BSA composites.

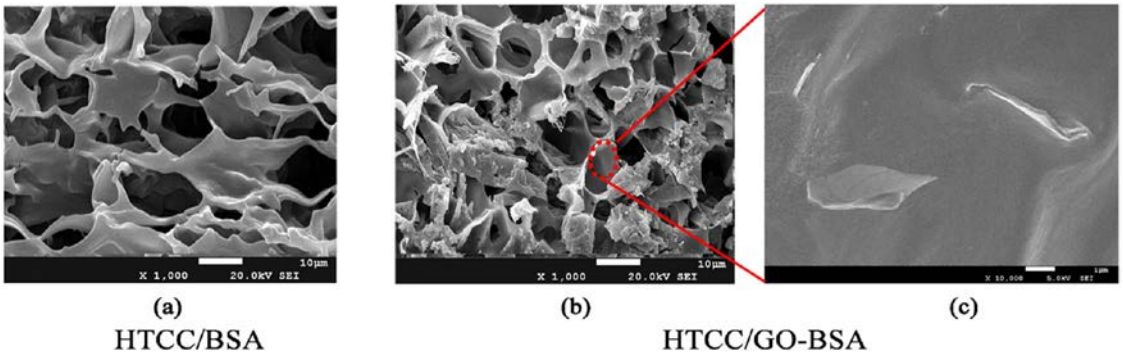

Fig. 9. SEM images (1000×) of (a) HTCC/BSA hydrogels (b) HTCC/2.0 wt%GO-BSA (c) images of HTCC/2.0 wt%GO-BSA with high magnification (10,000×).

Please cite this article in press as: X. Zhao, et al., Controlled pH- and glucose-responsive drug release behavior of cationic chitosan based nanocomposite hydrogels by using graphene oxide as drug nanocarrier, J. Ind. Eng. Chem. (2016), http://dx.doi.org/10.1016/j.jiec.2016.12.023

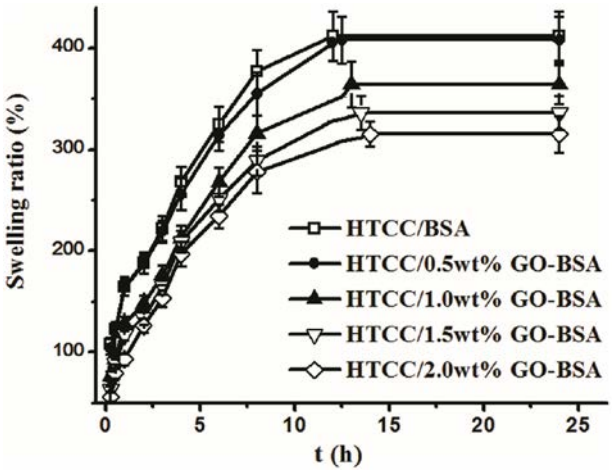

Fig. 10. Swelling ratios of HTCC/GO-BSA hydrogels with different GO-BSA content in buffer solutions (pH 6.8).

and more compact structure of the hydrogels with high content of GO-BSA.

pH-sensitive drug release behavior of HTCC/GO-BSA hydrogels

To investigate the effect of pH value of the external medium on the drug release behavior of HTCC/GO-BSA hydrogels, the cumulative release amount of BSA in PBS buffer solution with pH 6.8 and 7.4 was measured. Cumulative release data (as shown in Fig. 11) indicated that by increasing the pH value from 6.8 to 7.4, a considerable decrease in cumulative release was observed for all hydrogels, suggesting that the drug release profiles of all HTCC/GO-BSA hydrogels were pH-sensitive. With increasing GO-BSA content, the difference of the cumulative release in the medium of pH 6.8 and 7.4 became more and more significant, indicating an enhanced pH-sensitivity. Moreover, the release rate was obviously slowed down during the initial 5 h by the introduction of GO-BSA.

The drug release kinetics of HTCC/GO-BSA was studied with the following Korsmeyer–Peppas model:

$$\ln M_t/M_\infty = n\ln t + \ln k \quad (13)$$

where M_t/M_∞ is the fractional drug release at time t; k is a kinetic constant incorporating the structural characteristics of the matrix; and n is the release exponent, indicative of the drug release mechanism. In the case of Fickian release, n has the limiting value of 0.43. For case II, transport or relaxation controlled delivery, the exponent n is 0.85 [28,29]. The non-Fickian release or anomalous transport of drug occurred when the n values were between 0.43 and 0.85, which corresponds with the coupled diffusion/polymer relaxation.

As listed in Table 3, the correlation coefficient (r^2) approaching 0.98 was obtained for all hydrogels, indicating that the release data fitted well to the model. The exponent n values for the release of BSA from the hydrogel were all less than 0.43, suggesting a Fickian release behavior and that diffusion through the swelling of hydrogels was the main factor in controlling BSA release. The value of constant k for all HTCC/GO-BSA hydrogels in buffer solution with pH 6.8 was larger than that in buffer solution with pH 7.4, which indicated that the drug release of all HTCC/GO-BSA hydrogels were pH-sensitive. Moreover, in buffer solution with the same pH value, the constant k of hydrogels decreased with increasing GO-BSA content, which indicated that the release of BSA was slowed down by introduction of GO-BSA.

The pH-sensitive drug release behavior of HTCC/GO-BSA hydrogels should be attributed to a different hydrolysis degree in PBS buffer solution with pH 6.8 and pH 7.4, because the acidic environment could promote the hydrolysis of HTCC. At physiological condition (pH 7.4), the weak degree of ionization along with the less positively charged amine groups of HTCC and more hydrogen bonds resulted in a relatively dense network structure with pore size 4–8 μm (Fig. 12(a)) and restricting BSA release from its carrier. In contrast, the amine groups on the HTCC chains became protonated, forming the hydrophilic $—NH_3^+$ groups and $—N^+(CH_3)_3$ groups under a subacid environment (pH 6.8). The resulting electrostatic repulsion between the protonated cationic

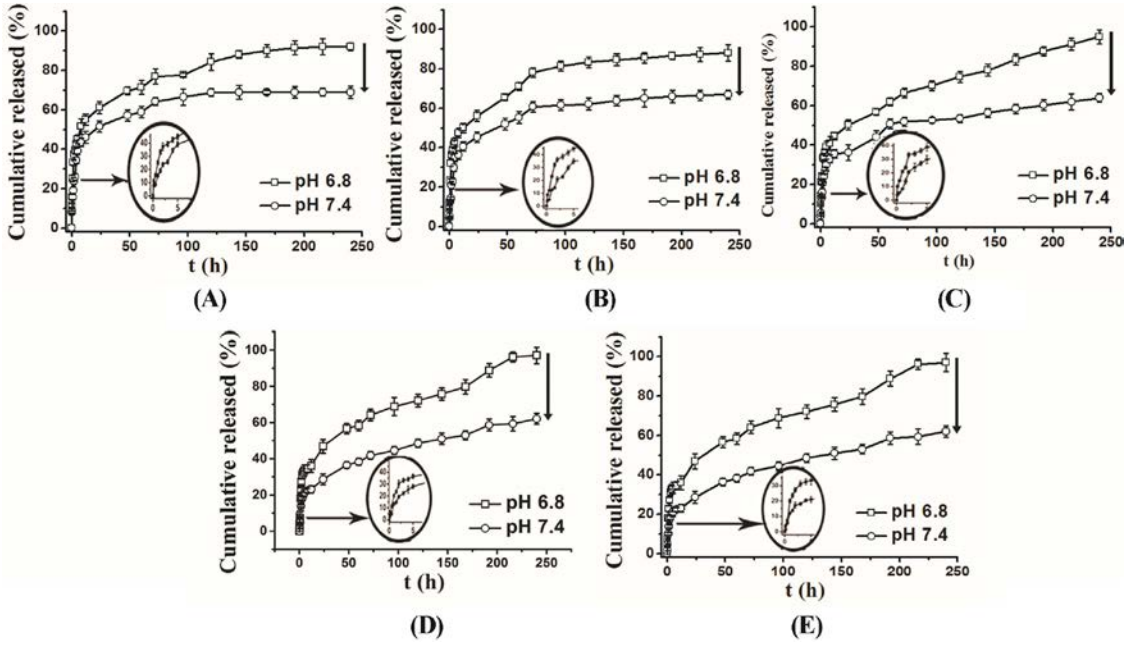

Fig. 11. pH-responsive release behavior of HTCC/GO-BSA hydrogels in different pH conditions (pH 6.8 and 7.4) at 37 °C (A-HTCC/BSA; B-HTCC/0.5 wt%GO-BSA; C-HTCC/1.0 wt% GO-BSA; D-HTCC/1.5 wt%GO-BSA; E-HTCC/2.0 wt%GO-BSA).

Please cite this article in press as: X. Zhao, et al., Controlled pH- and glucose-responsive drug release behavior of cationic chitosan based nanocomposite hydrogels by using graphene oxide as drug nanocarrier, J. Ind. Eng. Chem. (2016), http://dx.doi.org/10.1016/j.jiec.2016.12.023

Table 3
Drug release kinetic data for BSA-loaded modified chitosan hydrogels obtained from fitting drug release experimental data to the Korsmeyer–Peppas equation.

Samples	pH	Korsmeyer–Peppas model			Transport mechanism
		Correlation coefficient, r^2	Diffusion exponent, n	Kinetic constant, k	
HTCC/BSA	6.8	0.9810	0.2142	29.8574	Fickian diffusion
	7.4	0.9425	0.2199	22.9075	
HTCC/0.5 wt%GO-BSA	6.8	0.9706	0.2191	28.2306	Fickian diffusion
	7.4	0.9499	0.2455	18.9770	
HTCC/1.0 wt%GO-BSA	6.8	0.9871	0.2502	23.1590	Fickian diffusion
	7.4	0.9605	0.2507	16.5737	
HTCC/1.5 wt%GO-BSA	6.8	0.9867	0.2619	21.4180	Fickian diffusion
	7.4	0.9734	0.2536	15.6806	
HTCC/2.0 wt%GO-BSA	6.8	0.9804	0.2953	18.4620	Fickian diffusion
	7.4	0.9883	0.3034	11.4842	

groups weakened the intermolecular and intramolecular hydrogen bonding interaction of HTCC molecules, and the obvious loose network structure with pore size 10–15 μm (Fig. 12(b)) can be observed. As a result, the PBS buffer solution can diffuse into the HTCC/GO-BSA network easily, which would facilitate swelling and drug release.

The morphology of HTCC/BSA and HTCC-2.0wt%GO-BSA hydrogels after immersion in pH 6.8 PBS buffer solutions for 1 h was shown in Fig. 13. Due to the strong hydrogen bonding and electrostatic interactions between —COOH/—OH group on GO and $—NH_2$ group on HTCC, a more compact network structure formed by introduction of GO-BSA, which could slow down the initial burst release rate of hydrogels.

Glucose-responsive drug release behavior of HTCC/GO-BSA hydrogels

The pH-sensitive HTCC/GO-BSA hydrogels entrapped with GOD were used as a glucose responsive drug release system. Fig. 14(a) and (b) showed the cumulative release profiles of BSA from HTCC/BSA and HTCC/2.0 wt%GO-BSA hydrogels in response to different concentrations of glucose at pH 7.4, 37 °C, respectively. It was observed that, for both hydrogels, a much slower release rate was obtained when the hydrogels were exposed to the control solutions (0 mg ml^{-1}) and the basal glucose level (1 mg ml^{-1}) than that for the hyperglycemic glucose level (4 mg ml^{-1}), indicating an obvious glucose-sensitivity. Noticeably, the difference between BSA release profiles in the medium with glucose concentrations of 0 and 4 mg ml^{-1} was more significant for HTCC/2.0 wt%GO-BSA compared with HTCC/BSA hydrogel, indicating a more distinct glucose-sensitivity. Moreover, for HTCC/BSA hydrogels, a burst release behavior can be observed with different glucose concentrations during the initial 10 h. While for HTCC-2.0 wt%GO-BSA hydrogels, it exhibited a much lower initial burst release and a slower release rate compared with HTCC/BSA hydrogels.

The glucose-responsive drug release kinetics were studied with the Korsmeyer–Peppas model (Eq. (13)), and the related

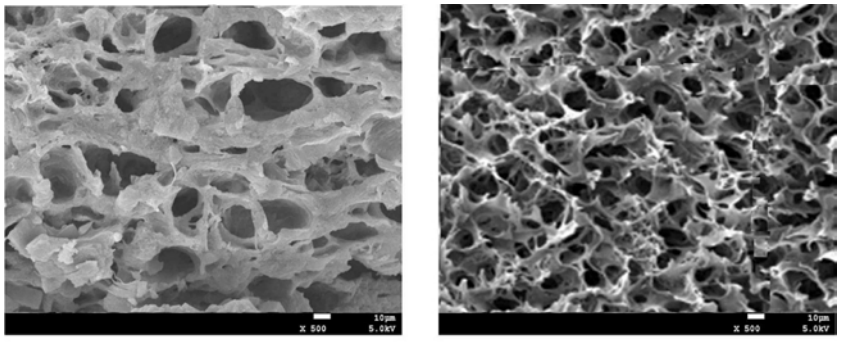

Fig. 12. SEM images (×500) of HTCC/2.0 wt%GO-BSA hydrogels after immersion in PBS buffer solution at 37 °C for 1 h. (a) At pH 6.8; (b) at pH 7.4.

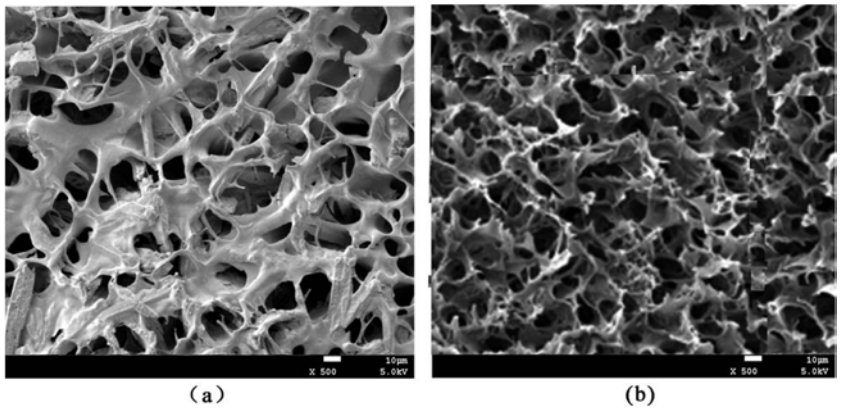

Fig. 13. SEM images (×500) of HTCC/GO-BSA hydrogels after immersion in pH 6.8 PBS buffer solution at 37 °C for 1 h (a) HTCC/BSA; (b) HTCC/2.0 wt%GO-BSA.

Please cite this article in press as: X. Zhao, et al., Controlled pH- and glucose-responsive drug release behavior of cationic chitosan based nanocomposite hydrogels by using graphene oxide as drug nanocarrier, J. Ind. Eng. Chem. (2016), http://dx.doi.org/10.1016/j.jiec.2016.12.023

Table 4
Drug release kinetic data for BSA-loaded HTCC/GO-BSA hydrogels in different glucose concentration obtained from fitting drug release experimental data to the Korsmeyer–Peppas equation.

Samples	Glucose concentration (mg/ml)	Korsmeyer–Peppas model			Transport mechanism
		Correlation coefficient, r^2	Diffusion exponent, n	Kinetic constant, k	
HTCC/BSA	0	0.9814	0.2445	9.5780	Fickian diffusion
	1	0.9517	0.1581	29.3573	Fickian diffusion
	4	0.9732	0.1881	32.0494	Fickian diffusion
HTCC/2.0 wt%GO-BSA	0	0.9659	0.3765	7.5235	Fickian diffusion
	1	0.9807	0.3984	8.4125	Fickian diffusion
	4	0.9897	0.3506	14.4611	Fickian diffusion

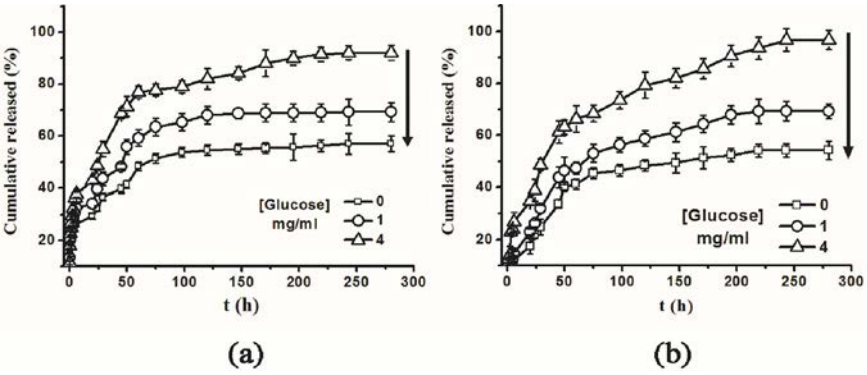

Fig. 14. Glucose responsive release behavior of HTCC/BSA hydrogels (a) and HTCC-2.0 wt%GO-BSA hydrogels (b) under different glucose concentrations: 0, 1, and 4 mg/ml at 37 °C.

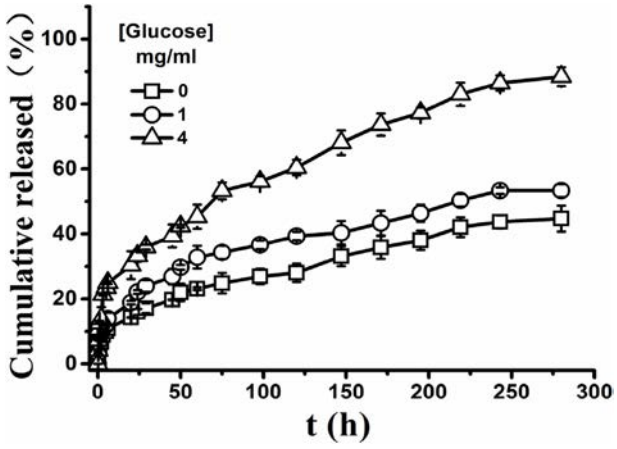

Fig. 15. Glucose responsive release behavior of HTCC/2.0 wt%GO-insulin hydrogels under different glucose concentrations: 0, 1, and 4 mg/ml at 37 °C.

parameters were listed in Table 4. A good correlation coefficient (r^2) approaching 0.98 was obtained in all cases. It was shown that the exponent n values for the release of BSA from HTCC hydrogels under different glucose concentrations were all less than 0.43, suggesting a Fickian release behavior. The values of constant k increased with an increase in glucose concentration, suggesting that HTCC/GO-BSA hydrogels showed obvious glucose sensitivity. Moreover, k value of HTCC-2.0 wt%GO-BSA hydrogels was much lower than that of HTCC/BSA hydrogels under same glucose concentrations, indicating that HTCC/2.0 wt%GO-BSA hydrogels may achieve a better slow-release effect.

Insulin, which was the conventional drug for diabetes, was used as the model drug, and HTCC/2.0 wt%GO-insulin drug delivery system was prepared. As shown in Fig. 15, the glucose responsive release behavior of HTCC/2.0 wt%GO-insulin hydrogel was similar with that of HTCC-2.0 wt%GO-BSA hydrogel. However, the release rate of the former was slightly slower than that of the latter.

Conclusions

In this study, GO was used as the drug nano-carrier and a series of GO-BSA intercalation complexes were prepared. With the increase of BSA/GO mass ratio, the interlayer spacing and intercalation ratio of GO-BSA increased, reaching the maximum and saturation at BSA/GO mass ratio of 8:1. The intercalation process of BSA into the GO layers was mainly driven by the mutual electrostatic interaction between negatively charged GO sheets and positively charged —NH_2 group on BSA chains. By using HTCC as the pH-sensitive polymer matrix, GOD as the glucose-sensitive receptor, GO-BSA loaded intelligent hydrogels were prepared. With increasing GO-BSA content, the storage modulus and crosslinking density of HTCC/GO-BSA hydrogel increased, which indicated that the introduction of GO-BSA resulted in a more-compact hydrogel. The release profiles revealed that all HTCC/GO-BSA hydrogels showed distinct pH-sensitivity, and the release of BSA from the hydrogel presented an almost Fickian release behavior. With the increase of GO-BSA content, the pH-sensitivity increased, and the initial release rate as well as constant k value decreased. An obvious glucose-sensitive drug release behavior can be observed for both HTCC/BSA and HTCC/2.0 wt%GO-BSA hydrogel. Compared with HTCC/BSA hydrogels, HTCC/2.0 wt%GO-BSA hydrogels exhibited a more distinct glucose-sensitivity and a much lower initial burst release.

References

[1] Z. Gu, A.A. Aimetti, Q. Wang, T.T. Dang, Y. Zhang, O. Veiseh, H. Cheng, R.S. Langer, D.G. Anderson, ACS Nano 7 (2013) 4194.
[2] X. Chen, W. Wu, Z. Guo, Z. Guo, J. Xin, J. Li, Biomaterials 32 (2011) 1759.
[3] J. Luo, S. Cao, X. Chen, X. Chen, S. Liu, H. Tan, W. Wu, J. Li, Biomaterials 33 (2012) 8733.
[4] S.I. Kang, Y.H. Bae, J. Control. Release 86 (2003) 115.

Please cite this article in press as: X. Zhao, et al., Controlled pH- and glucose-responsive drug release behavior of cationic chitosan based nanocomposite hydrogels by using graphene oxide as drug nanocarrier, J. Ind. Eng. Chem. (2016), http://dx.doi.org/10.1016/j.jiec.2016.12.023

[5] M.K.L. Chu, J. Chen, C.R. Gordijo, S. Chiang, A. Ivovic, K. Koulajian, Y. Sun, Lab Chip 12 (2012) 2533.
[6] J. Wu, Z.G. Su, G.H. Ma, Int. J. Pharm. 315 (2006) 1.
[7] K.Z. Elwakeel, M.A.A. El-Ghaffar, S.M. El-kousy, H.G. El-Shorbagy, Chem. Eng. J. 203 (2012) 458.
[8] X. Zou, X. Zhao, L. Ye, J. Ind. Eng. Chem. 21 (2015) 1389.
[9] X. Zou, X. Zhao, L. Ye, Chem. Eng. J. 273 (2015) 92.
[10] W.F. Lee, Y.T. Fu, J. Appl. Polym. Sci. 89 (2003) 3652.
[11] Q. Yuan, J. Shah, S. Hein, R.D.K. Misra, Acta Biomater. 6 (2010) 1140.
[12] X. Zhang, Z. Hui, D. Wan, H. Huang, J. Huang, H. Yuan, J. Yu, Int. J. Biol. Macromol. 47 (2010) 389.
[13] X. Yang, X. Zhang, Z. Liu, Y. Ma, Y. Huang, Y. Chen, J. Phys. Chem. C 112 (2008) 17554.
[14] X. Yang, Y. Wang, X. Huang, Y. Ma, Y. Huang, R. Yang, H. Duan, Y. Chen, J. Mater. Chem. 21 (2011) 3448.
[15] Z. Liu, J.T. Robinson, X. Sun, H. Dai, J. Am. Chem. Soc. 130 (2008) 10876.
[16] X. Yang, X. Zhang, Z. Liu, Y. Ma, Y. Huang, Y. Chen, J. Phys. Chem. C 112 (2008) 17554.
[17] S. Liu, L. Wang, J. Tian, Y. Luo, X. Zhang, X. Sun, J. Colloid Interface Sci. 363 (2011) 615.
[18] S. Liu, J. Tian, L. Wang, Y. Luo, X. Sun, Catal. Sci. Technol. 2 (2012) 339.
[19] J. Tian, R. Ning, Q. Liu, A.M. Asiri, A.O. Al-Youbi, X. Sun, ACS Appl. Mater. Interfaces 6 (2014) 1011.
[20] R. Ning, J. Tian, A.M. Asiri, A.H. Qusti, A.O. Al-Youbi, X. Sun, Langmuir 29 (2013) 13146.
[21] J. Tian, S. Liu, H. Li, L. Wang, Y. Zhang, Y. Luo, X. Sun, RSC Adv. 2 (2012) 1318.
[22] R. Justin, B. Chen, Carbohydr. Polym. 103 (2014) 70.
[23] Y. Chen, Y. Qi, X. Yan, H. Ma, J. Chen, B. Liu, Q. Xue, J. Appl. Polym. Sci. 131 (2014) 1 40006.
[24] F. Chambon, H.H. Winter, J. Rheol. 31 (1987) 683.
[25] M. Aliaghaie, H. Mirzadeh, E. Dashtimoghadam, S. Taranejoo, Soft Matter 8 (2012) 7128.
[26] M.J. Moura, M.M. Figueiredo, M.H. Gil, Rheological study of genipin cross-linked chitosan hydrogels, Biomacromolecules 8 (2007) 3823.
[27] Z. Lian, L. Ye, J. Appl. Polym. Sci. 128 (2013) 3325.
[28] O. Zamoume, S. Thibault, G. Regnié, M.O. Mecherri, M. Fiallo, P. Sharrock, Mater. Sci. Eng. C 31 (2011) 1352.
[29] A. Tabak, N. Yilmaz, E. Eren, B. Caglar, B. Afsin, A. Sarihan, Chem. Eng. J. 174 (2011) 281.

Please cite this article in press as: X. Zhao, et al., Controlled pH- and glucose-responsive drug release behavior of cationic chitosan based nanocomposite hydrogels by using graphene oxide as drug nanocarrier, J. Ind. Eng. Chem. (2016), http://dx.doi.org/10.1016/j.jiec.2016.12.023